Voltage-Dependent Blockade of Diverse Types of Voltage-Gated Ca^{2+} Channels Expressed in *Xenopus* Oocytes by the Ca^{2+} Channel Antagonist Mibefradil (Ro 40–5967)

I. BEZPROZVANNY and R. W. TSIEN

Department of Molecular and Cellular Physiology, Stanford University Medical Center, Stanford, California 94305

SUMMARY

Four different types of Ca^{2+} channel $\alpha1$ subunits, representing the major classes of voltage-gated Ca^{2+} channels, were individually coexpressed along with $\alpha2/\delta$ and $\beta2b$ subunits in *Xenopus* oocytes. These subunits (and the encoded channel types and major tissues of origin) included $\alpha1C$ (L-type, cardiac), $\alpha1B$ (N-type, central nervous system), $\alpha1A$ (P/Q-type, central nervous system), and $\alpha1E$ (most likely R-type, central nervous system). Divalent cation currents through these channels (5 mM Ba^{2+}) were evaluated with the two-microelectrode voltage-clamp technique. The expressed channels were compared with regard to their responses to a structurally novel, nondihydropyridine compound, mibefradil (Ro 40–5967). In the micromolar concentration range, this drug exerted clear inhibitory effects on each of the four channel types, reducing divalent cation current at all test potentials, with the non-L-type channels being more sensitive to inhibition than the L-type channels under fixed experimental conditions. For all channel types, mibefradil was a much more effective inhibitor at more depolarized holding potentials, suggesting tighter binding of the drug to the inactivated state than to the resting state. The difference in apparent affinities of resting and inactivated states of the channels, calculated based on a modulated receptor hypothesis, was 30–70-fold. In addition, the time course of decay of Ca^{2+} channel current was accelerated in the presence of drug, consistent with open channel block. The effect of increasing stimulation frequency was tested for L-type channels and was found to greatly enhance the degree of inhibition by mibefradil, consistent with promotion of block by channel opening and inactivation. Allowing for state-dependent interactions, the drug concentrations found to block L-, N-, Q-, and R-type channels by 50% are at least 10-fold higher than half-blocking levels previously reported for T-type channels in vascular smooth muscle cells under similar experimental conditions. This may help explain the ability of the drug to spare working myocardium (strongly negative resting potential, dominance of L-type channels in their resting state) while reducing contraction in blood vessels (presumably involving T-type channels or partially inactivated L-type channels). Thus, mibefradil is a new addition to the family of nonselective organic Ca^{2+} channel inhibitors, as exemplified by bepridil and fluspirilene, and may prove useful as an experimental tool for studying diverse physiological events initiated by Ca^{2+} influx. It complements classes of drugs with relatively selective effects on L-type channels, as exemplified by nifedipine and diltiazem.

Pharmacological agents have been very important in the identification of multiple classes of voltage-gated Ca^{2+} channels (1–8). Compounds that block or enhance various channel types have facilitated analysis with electrophysiological recordings and molecular cloning. Together, these approaches have led to the identification of at least six distinct types of voltage-gated Ca^{2+} channel in mammalian cells (9–12). New knowledge of Ca^{2+} channel diversity has been accompanied by increasing demand for a wide spectrum of pharmacological agents to help delineate the contributions of the channels in physiological settings. However, few agents are available to inhibit the more recently discovered classes

of Ca^{2+} channels. Current efforts have focused on peptide neurotoxins and small organic compounds, each with their own advantages and disadvantages. Peptide neurotoxins such as ω-CTx GVIA or ω-agatoxin IVA often provide considerable specificity for individual channel types (7) but are expensive, available in only limited quantities, and difficult to deliver to central nervous system targets that require penetration of an intact blood-brain barrier. Small organic molecules are much easier to obtain and deliver, but the drugs available have been strongly selected for their relative specificity for L-type channels (13); well-known examples are nifedipine or diltiazem. In comparison, little is known about organic inhibitors for non-L-type channels, although recently several nonselective Ca^{2+} channel inhibitors have emerged, as exemplified by bepridil and fluspirilene (14–16).

ABBREVIATIONS: ω-CTx, ω-conotoxin; HVA, high-voltage-activated; HEPES, 4-(2-hydroxyethyl)-1-piperazineethanesulfonic acid;

Mibefradil (Ro 40–5967) is a new nondihydropyridine calcium antagonist (Hoffmann-La Roche) that has demonstrated the ability to decrease blood pressure without a biologically relevant negative inotropic effect on myocardium (17). These characteristics have been supported in both animal studies and clinical trials, suggesting the usefulness of this compound for the treatment of hypertension. Despite the significant clinical potential of the drug, very little is known about its molecular mechanisms of action. Binding studies have shown that mibefradil inhibits binding of [³H]desmethoxyverapamil to cardiac membranes but does not affect the binding of dihydropyridines, suggesting an interaction with the phenylalkylamine site of L-type cardiac channels (18). It was also demonstrated in electrophysiological experiments that mibefradil inhibited inward L-type Ca^{2+} currents in isolated cardiomyocytes (19). Recently, it was shown that mibefradil may act in the submicromolar range to inhibit T-type Ca^{2+} channels in vascular smooth muscle cells (20). The block of T-type channels is much more potent than that of L-type channels (20, 21).

The recent availability of cloned subunits of various voltage-gated Ca^{2+} channels opens up the possibility of characterizing actions of new pharmacological agents on individual channel types in the virtual absence of contaminating currents. In fact, there has been no systematic comparison of the characteristics of class C, B, A, and E $\alpha 1$ subunits under identical conditions of expression. We report the results of such a comparison, along with a systematic analysis of the effects of mibefradil on the various channel types. Each class of $\alpha 1$ subunit was individually coexpressed with $\alpha 2/\delta$ and $\beta 2b$ subunits in Xenopus oocytes and supported divalent cation currents, which were recorded with the two-microelectrode voltage-clamp technique. The resulting Ca^{2+} channel currents displayed properties similar to L-, N-, Q-, and R-type currents in mammalian cells and provided the opportunity to study the effects of mibefradil on individual components in isolation. Mibefradil inhibited each of the four channel types. The channels derived from neuronal sources (N-, Q-, and R-type) tended to be more sensitive to inhibition than cardiac L-type channels. For all channel types, mibefradil was more effective at depolarized holding potentials, indicating a higher affinity binding of the drug to the inactivated state; blockade was also promoted by channel opening. Thus, mibefradil provides a clear example of an organic Ca^{2+} channel blocker that acts on N-, Q-, and R-type channels with prominent use and voltage dependence, characteristics previously described for blockade of L-type channels.

Materials and Methods

Preparation of Xenopus oocytes and cRNA injections. Female Xenopus laevis were anesthetized by immersion in 0.2% tricaine methanesulfonate for ~40 min before surgery. Ovarian tissue was removed via a small incision in the abdomen and chopped with scissors in Ca^{2+}-free OR-2 solution (82.5 mM NaCl, 2 mM KCl, 1 mM MgCl₂, 5 mM HEPES, pH 7.5). Single stage V–VI oocytes free of follicular cells were obtained by incubation with shaking for 2 hr in OR-2 containing 2 mg/ml collagenase A (Boehringer Mannheim), as described previously (22). After collagenase treatment, oocytes were washed several times in OR-2 and then transfered to ND96 medium (96 mM NaCl, 2 mM KCl, 1.8 mM CaCl₂, 1 mM MgCl₂, 5 mM HEPES, pH 7.6) supplemented with 2.5 mM sodium pyruvate and antibiotics

(gentamacin or penicillin/streptomicin mixture) and sorted manually under a dissecting microscope. Selected oocytes were maintained at 18° for several hours or days before cRNA injection.

RNA species encoding voltage-gated Ca^{2+} channel subunits were synthesized by in vitro transcription procedure with the use of bacteriophage T7 or SP6 RNA polymerases by following standard protocol (23). The integrity of the resulting cRNA was tested by gel electrophoresis in the presence of 18% formaldehyde. The concentration of cRNA was estimated based on the intensity of ethidium bromide staining of the corresponding band compared with the staining of a standard 1-kb RNA ladder (GIBCO-BRL). The following clones were used as DNA templates for cRNA synthesis: rabbit cardiac $\alpha 1C$ (24), human brain $\alpha 1B$ chimeric construct (25), rabbit brain $\alpha 1A$ (26), human brain $\alpha 1E$ (obtained from Neurex Corp.), rabbit skeletal muscle $\alpha 2/\delta$ (provided by T. Tanabe and S. Numa, Kyoto University Faculty of Medicine, Kyoto Japan), and rabbit heart $\beta 2b$ (27).

Expression of various types of voltage-gated Ca^{2+} channels in oocytes was achieved by injection of the appropriate $\alpha 1$ cRNA species, plus $\alpha 2/\delta$ cRNA and $\beta 2b$ cRNA, dissolved in water in an approximate molar ratio of 1:1:1. The average volume injected was ~50–100 nl/oocyte, which corresponds to 5–10 ng of the cRNA mixture per oocyte based on the concentration of cRNA used for injections. Injected oocytes were maintained at 18° for several weeks in ND96 solution supplemented with sodium pyruvate and antibiotics.

Electrophysiological recordings and data analysis. For current measurements, oocytes were placed in 5 mM Ba^{2+} recording solution [5 mM Ba(OH)₂, 2 mM KOH, 85 mM tetraethylammonium, 5 mM HEPES, pH adjusted to 7.4 with methanesulfonic acid]. Chloride salts were not included in this solution to minimize the currents through endogenous Cl⁻ channels present in the Xenopus oocytes. The chamber containing the oocytes was continuously perfused with fresh 5 mM Ba^{2+} recording solution at a flow rate of ~1 ml/min. The 10 mM stock solution of mibefradil (Ro 40–5967; Hoffmann-La Roche Ltd.) in water was maintained at room temperature for 2–3 weeks after preparation. This stock of mibefradil was diluted to the desired concentration of the drug (1–100 μM) in 5 mM Ba^{2+} recording solution immediately before electrophysiological experiments. Application of mibefradil to oocytes was achieved by perfusion of recording chamber with the 5 mM Ba^{2+} solution containing the desired drug concentration.

Whole-cell Ba^{2+} currents in oocytes were recorded using a two-electrode voltage-clamp amplifier (Model OC-725A, Warner Instruments). Both current-passing and voltage-measuring electrodes were filled with 3 M KCl and had resistances in the range of 0.5–5 MΩ. The electrical potential of the solution in the bath was measured with a Ag/AgCl pellet immersed in the small reservoir filled with 3 M KCl and connected to the recording chamber by a 3 M KCl-agar bridge. Clamp current injected by intracellular current electrode was measured with a separate bath-clamp circuit connected to the recording chamber via chlorided silver wire placed directly in the bath. Ca^{2+} channel openings were induced by step depolarizations from holding potential to test potential every 15 sec unless otherwise noted (see Results). The test pulse duration was 150 msec, or 50 msec in some experiments. The current signal was filtered at 500 Hz, sampled at 2 kHz with an analog-to-digital converter (Axon Instruments Inc.) and stored on the hard drive for data analysis. Occasional leak traces were taken during each experiment with a P/6 protocol, and linear leak and capacitance transients were subtracted off-line during the course of subsequent data analysis. Residual spikes of current at the beginning and end of each current trace left after the subtraction procedure were blanked in the current records as presented. Computer programs for data acquisition and analysis were written in AxoBasic. All experiments were conducted at room temperature (21–23°).

Results

Mibefradil inhibits multiple types of voltage-gated Ca²⁺ channels. Fig. 1 shows representative two-electrode voltage-clamp recordings of currents passing through the voltage-gated Ca^{2+} channels resulting from four different $\alpha 1$ subunits. The $\alpha 1$ subunits (indicated in Fig. 1) were individually coexpressed with $\beta 2b$ and $\alpha 2/\delta$ subunits in *Xenopus* oocytes. Channel activity was evoked every 15 sec by a 150-msec pulse from the -80 mV holding potential to a test potential of 0 mV ($\alpha 1C$, $\alpha 1B$, and $\alpha 1A$ clones) or $+10$ mV ($\alpha 1E$ clone). Divalent cation inward currents through the channels were recorded with 5 mM Ba^{2+} as the charge carrier in the bathing solution. Channels do not inactivate substantially during 150-msec test pulse, as previously reported for the $\beta 2b$ subunit (22). The inward current through all four channel types was decreased in magnitude by exposure to 10 μM mibefradil and further diminished when the drug concentration was increased to 100 μM (Fig. 1).

Fig. 2 shows the relationship between peak current and test potential in the absence of drug and in the presence of 10

○ control

● 10 μM mibefradil

▲ 100 μM mibefradil
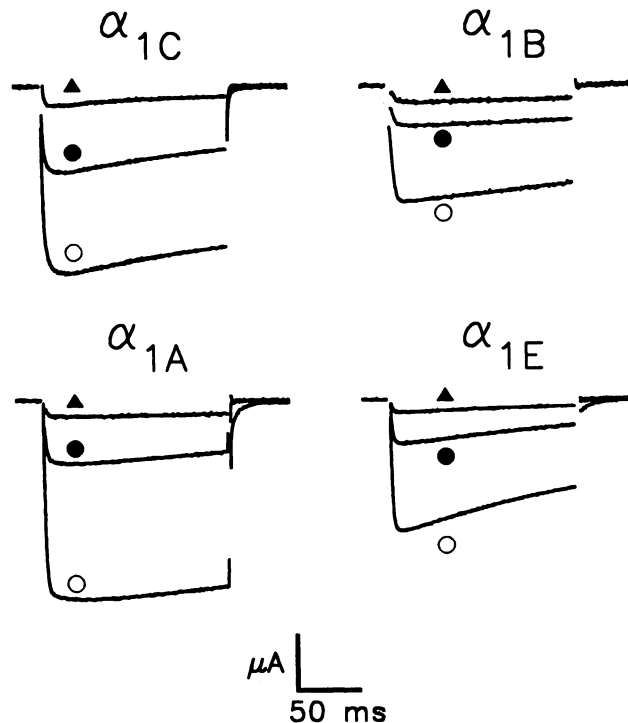
Fig. 1. Mibefradil inhibits multiple types of voltage-gated Ca^{2+} channels expressed in *Xenopus* oocytes. Four major classes of HVA Ca^{2+} channel $\alpha 1$ subunits (C-, B-, A-, and E-type) were expressed in *Xenopus* oocytes in combination with $\alpha 2/\delta$ and $\beta 2b$ subunits. Whole-cell Ba^{2+} currents were evoked by 150-msec step depolarizations from -80 mV holding potential to 0 mV (α_{1C}, α_{1B}, and α_{1A}) or $+10$ mV (α_{1E}). The effect of 10 μM and 100 μM of mibefradil on recorded currents is shown. Currents were leak-subtracted off-line, and capacitance transient artifacts were blanked from the traces shown. *Vertical scale bar* corresponds to 0.5 μA for $\alpha 1C$, $\alpha 1B$, and $\alpha 1E$ and 1 μA for $\alpha 1A$.

○ control
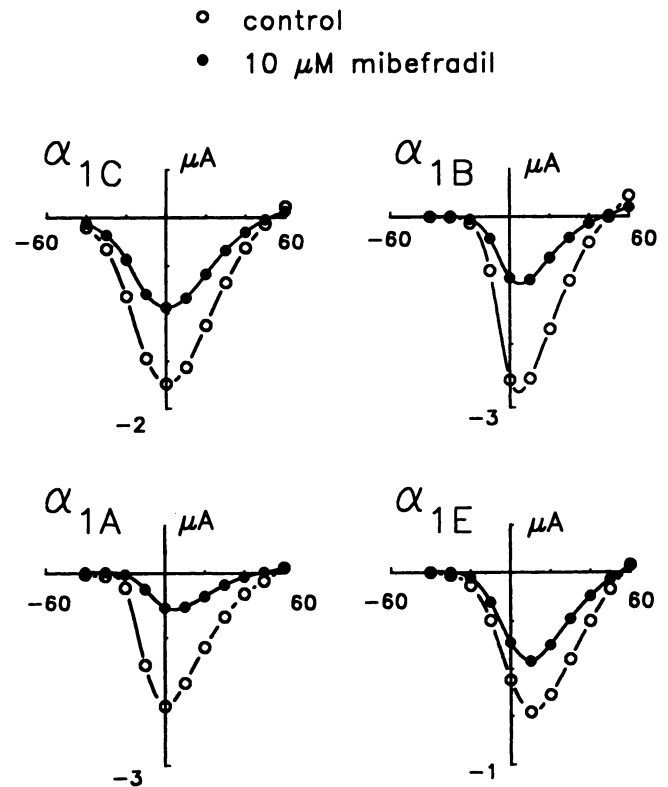
● 10 μM mibefradil

Fig. 2. Voltage dependence of peak current of class C, A, B, and E $\alpha 1$ subunits in the presence and absence of 10 μM mibefradil. Oocytes were held at -60 mV (α_{1A}), -80 mV (α_{1C} and α_{1B}), or -100 mV (α_{1E}) holding potentials. Peak current-voltage relationships were obtained by changing test pulse potentials from -40 mV to $+60$ mV in 10-mV increments. The peak currents measured at every test potential in control conditions (●) and in the presence of 10 μM mibefradil (○) are plotted against the value of test potential used. *Curves*, drawn using a cubic spline routine.

μM mibefradil for each of the four channel types. No significant current was observed at test potentials more negative than -30 mV, which is consistent with the classification of each of the four subunits as an HVA Ca^{2+} channel. For all four $\alpha 1$ subunits, the reversal potential was ~+55 mV and was unaffected by the presence of mibefradil (Fig. 2). The peak inward current was maximal at a test potential of 0 mV for the $\alpha 1C$, $\alpha 1B$, and $\alpha 1A$ subunits and at $+10$ mV for the $\alpha 1E$ subunit. The inward maximum of the current-voltage relationship was not shifted by the drug in any case. In the results that follow, the effects of mibefradil were evaluated at a test potential corresponding to the peak of the current-voltage relationship.

Dose-dependence of mibefradil block. The concentration-dependence of the blockade by mibefradil was studied more systematically by application of gradually increasing doses of the drug over the range of 1–100 μM (Fig. 3). The holding potential was set to -80 mV, and inward currents were evoked by short (50 or 150 msec) depolarizing pulses, applied once every 15 sec. Fig. 3A shows representative experiments for each channel type. Peak current amplitudes for each pulse were normalized to the value in the absence of drug and plotted against time. Each stepwise increase in the concentration of mibefradil caused a sharply defined decline in peak current amplitude. Removal of the drug near the end

A

B
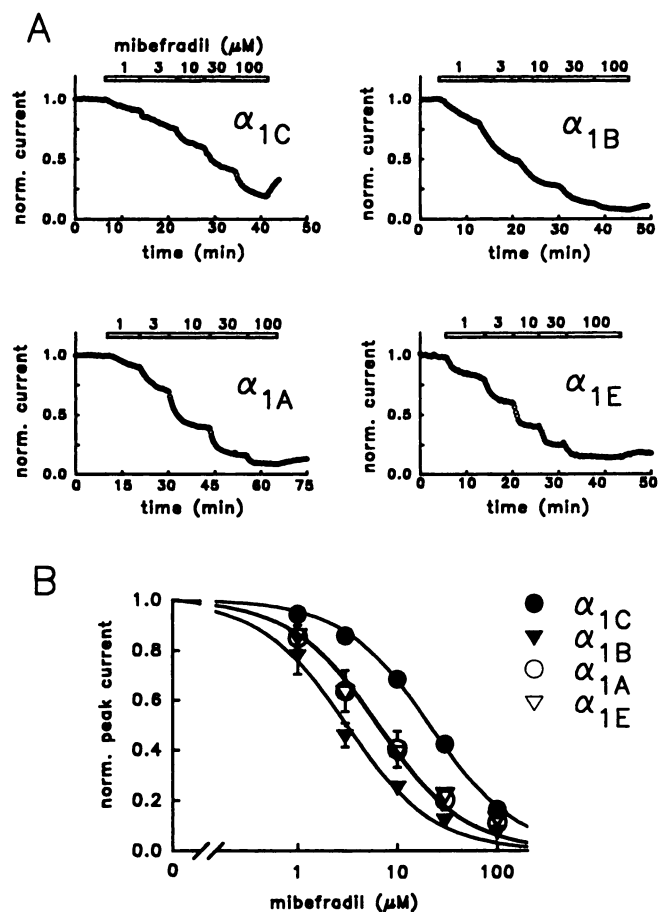
Fig. 3. Concentration dependence of mibefradil block (holding potential, −80 mV). A, Representative experiments illustrating approach for determining dose-dependence of mibefradil effect. Inward currents were induced by depolarization to 0 mV (α_{1C}, α_{1B}, and α_{1A}) or +10 mV (α_{1E}) every 15 sec. Concentration of mibefradil in the recording medium was increased from 1 μM to 100 μM during the course of the experiment. Peak current amplitudes, measured after near-steady state was reached at every mibefradil concentration, were normalized to the peak current amplitude in the absence of the drug. B, Cumulative dose-response relationships. Data from at least four experiments were normalized individually and then pooled for each class of α1 subunit and plotted as mean ± standard error with symbols as designated. Curves, best fits to the data using a one-to-one binding curve according to the equation $1/(1 + [\text{mibefradil}]/K_d)$. Values of K_d, the apparent dissociation constant, were 21.0 μM for α1C, 3.1 μM for α1B, 6.3 μM for α1A, and 6.5 μM for α1E.

of the experiment led to a partial recovery of current size for all channel types.

The cumulative dose-response curves for block by mibefradil are plotted in Fig. 3B. Compiled data for each class of α1 subunit were closely fitted with smooth curves representing one-to-one binding of mibefradil to individual channels. Values of the apparent dissociation constant (K_d) were 22 ± 3 μM (five experiments) for α1C, 3 ± 1 μM (three experiments) for α1B, 8 ± 3 μM (six experiments) for α1A, and 7 ± 1 μM (three experiments) for α1E. Thus, L-type Ca²⁺ channels generated by α1C derived from cardiac tissue are much less sensitive to inhibition than their neuronally derived counterparts. Among the latter, N-type channels encoded by α1B subunit (28) were significantly more sensitive to inhibition by mibefradil than the channels supported by α1A subunits

(possibly Q-type) (22) and α1E subunits (possibly R-type) (8, 29, 30).

Blockade by mibefradil depends on holding potential. In all experiments described so far, the effects of mibefradil on expressed Ca²⁺ channels were evaluated at a fixed holding potential of −80 mV. This is important to bear in mind because the holding potential level is known to influence the potency of nitrendipine and other dihydropyridine antagonists in blocking L-type Ca²⁺ channels (31, 32) and of fluspirilene in blocking P-type channels (14). It has been shown that steady depolarization promotes high affinity binding of dihydropyridines to cardiac channels, very likely by causing channels to enter an inactivated state in which they bind the drug very tightly (33). To determine whether similar behavior is observed for mibefradil, we conducted experiments in which the blockade by a fixed concentration of drug (10 μM) was evaluated at different holding potentials.

A

B
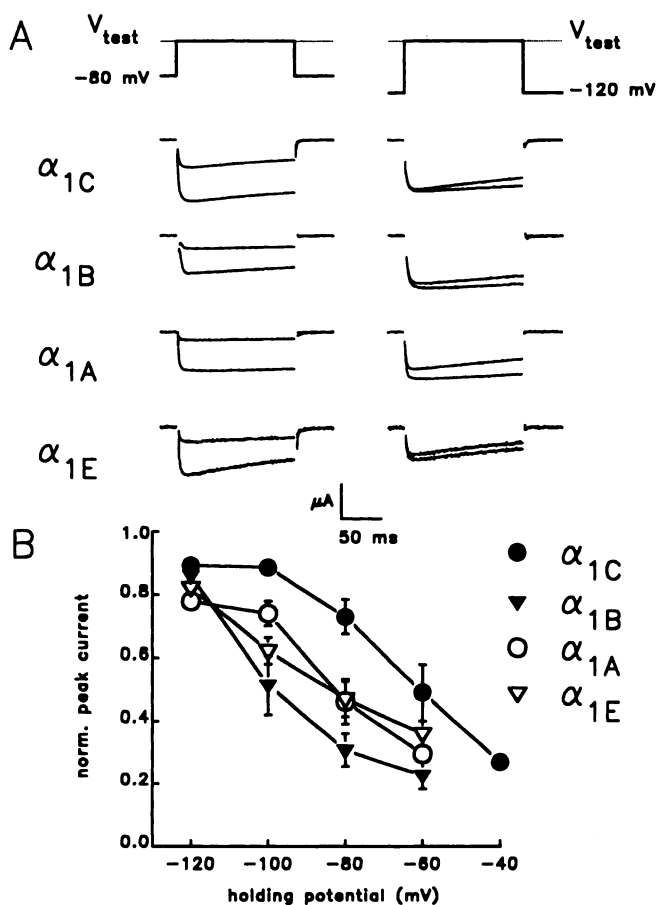
Fig. 4. The degree of Ca²⁺ channel inhibition by mibefradil depends on holding potential. A, Comparison of inward currents evoked from −80 mV (left) or −120 mV (right) holding potentials (150-msec depolarizing pulses, 10 μM mibefradil). Test potential was 0 mV (α_{1C}, α_{1B}, and α_{1A}) or +10 mV (α_{1E}). Vertical scale bar corresponds to 1 μA for α1C, α1B, and α1A and 0.25 μA for α1E. B, Fraction of the current resistant to inhibition by 10 μM mibefradil as a function of holding potential. Size of the the peak current in the presence of 10 μM mibefradil was expressed as a fraction of the peak current before the addition of the drug in individual oocytes. Each point represents mean ± standard error of values obtained for each class of α1 subunit from at least three independent experiments at each holding potential. Occasionally, experiments at two different holding potentials were performed with the same oocyte, with drug washed out between runs.

Fig. 4A shows representative current traces from this series of experiments for each channel type. Currents were evoked by depolarizing pulses from holding potentials of −80 mV and −120 mV before and after application of 10 μM mibefradil. It is evident that for every channel type, blockade by the drug is much more pronounced if the holding potential is set at −80 mV than at −120 mV.

Fig. 4B shows pooled results from this series of experiments over the range of holding potentials between −120 mV and −60 mV (−40 mV for the α1C subunit). The peak current amplitude in the presence of 10 μM mibefradil was normalized by the control value before addition of the drug and then averaged for multiple experiments. It is clear that the inhibitory effect of mibefradil increases markedly as the holding potential is displaced toward less-negative voltages. Although all four channel types display this pattern of behavior, the expressed α1C subunits (cardiac L-type channels) are blocked to a lesser degree than the neuronally derived channels at any given holding potential.

Quantitative implications based on the modulated receptor hypothesis. One possible explanation for these results is that mibefradil binds preferentially to the inactivated state of the channels and much more weakly to the resting state, following the modulated receptor hypothesis (34–36). We begin by considering only resting (R) and inactivated (I) states of the channel, a simplification that proved useful in the analysis of effects of lidocaine on Na⁺ channels (37) and nitrendipine on Ca²⁺ channels (32). For this model, the apparent dissociation constant of the drug (K_{app}, μM) can be expressed in terms of K_R and K_I, the dissociation constants for drug binding to resting and inactivated states of the channel, and $h_\infty(V)$, the fraction of the channels in the resting (noninactivated) state in the absence of the drug (32, 37):

$$K_{app}^{-1}(V) = [h_\infty(V) \cdot K_R^{-1}] + \{[1 - h_\infty(V)] \cdot K_I^{-1}\} \quad (1)$$

Because the interaction between mibefradil and the Ca²⁺ channel appears to be one-to-one (Fig. 3B), the fraction of the current that remains in the presence of the drug [q(V)] is derived as follows:

$$q(V) = 1/(1 + [Ro]K_{app}^{-1}) = 1/[1 + \{[Ro]h_\infty(V) \cdot K_R^{-1}\} \quad (2)$$
$$+ \{[Ro][1 - h_\infty(V))] \cdot K_I^{-1}\}]$$

where [Ro] is the concentration of mibefradil (10 μM in the data shown in Fig. 4B). For a maintained holding potential of −120 mV, virtually all channels are presumed to occupy the resting state ($h_\infty = 1$) and, therefore:

$$q(-120) = 1/(1 + [Ro]K_R^{-1}) \quad (3)$$

Thus, K_R can be determined. K_I can be estimated from data obtained at a less-negative holding potential, where $h_\infty < 1$. For example, at −80 mV, q(−80), the fraction of current that remains in the presence of drug will be smaller because of preferential binding to the inactivated state as well as the resting state. Accordingly, the apparent dissociation constant at −80 mV, $K_{app}(-80)$, will decrease to a lower concentration than K_R, in agreement with eq. 1:

$$K_{app}^{-1}(-80) = [h_\infty(-80) \cdot K_R^{-1}] + \{[1 - h_\infty(-80)] \cdot K_I^{-1} \quad (4)$$

To determine the fraction of channels in the inactivated state, we began by measuring peak currents evoked by repetitive depolarizations (every 30 sec) to a fixed test potential from different holding potentials. The holding potential was set at −120 mV in the beginning of an experiment and was progressively elevated to increasingly depolarized levels, with two test pulses from each holding potential. The data obtained with this "cumulative inactivation" protocol were fit with a Boltzmann relationship (Fig. 5A). During the course of these experiments, we noticed that over an intermediate range of holding potentials, the second test pulse consistently evoked a somewhat smaller current than the first test pulse from the same holding potential. This indicated that even 30 sec at a given holding potential is not a sufficient period for the channels to achieve a true steady state; thus, the fraction of channels in the inactivated state in Fig. 5A would be an underestimate relative to true steady state conditions.

To estimate $h_\infty(-80)$ more precisely, we conducted a series of experiments illustrated in Fig. 5B. The holding potential was kept at −80 mV for several minutes and then suddenly switched to −120 mV. Test currents were evoked by depolarizing pulses to a fixed test potential every 15 sec until a true steady state was reached; this required maintaining the holding potential at specific levels for several minutes. The ratio of the peak currents evoked at steady state at each test potential, I(−80)/I(−120), was taken as a measure of $h_\infty(-80)$. The values obtained for α1 subunit classes A, B, C, and E were 0.90 ± 0.02 (five experiments), 0.75 ± 0.04 (five experiments), 0.95 ± 0.01 (three experiments), and 0.78 ± 0.01 (four experiments), respectively. Although appropriate for comparison with drug-induced blockade, this approach differs from conventional protocols used to measure the degree of inactivation, which typically use conditioning prepulses lasting several seconds. Even with 1-min periods at depolarized levels (Fig. 5A), the estimates of "steady state" inactivation are different from those obtained with longer sojourns.

By application of eqs. 3 and 4, the dissociation constants of mibefradil binding to resting (K_R) and inactivated (K_I) conformations of the channel were estimated for each clone (Table 1). The values of K_I must be regarded as approximate because of the difficulties of estimating $h_\infty(V)$ in the face of slow inactivation. However, the analysis leads to interesting conclusions. First, the dissociation constant for mibefradil in the inactivated state is ~30–70 times lower than that in the resting state. Second, the dissociation constants of resting and inactivated states are very similar for all four clones. Evidently, the main reason that the cardiac α1C clone appears to be less sensitive to inhibition by mibefradil (see Figs. 3 and 4) is that this channel type inactivates at more positive holding potentials compared with the neuronally derived subunits (Fig. 5).

State-dependent changes in the rate of mibefradil dissociation. Additional support for the hypothesis that mibefradil binds preferentially to the inactivated state of the channels comes from the observation that the rate of drug washout was accelerated dramatically by switching to more hyperpolarized holding potential. This phenomenon is illustrated by Fig. 6. In this experiment, α1A channels were inhibited by the addition of 10 μM mibefradil in the bathing medium at holding potential equal to −80 mV. When mibefradil was removed from the bathing medium, some reversal

A

B
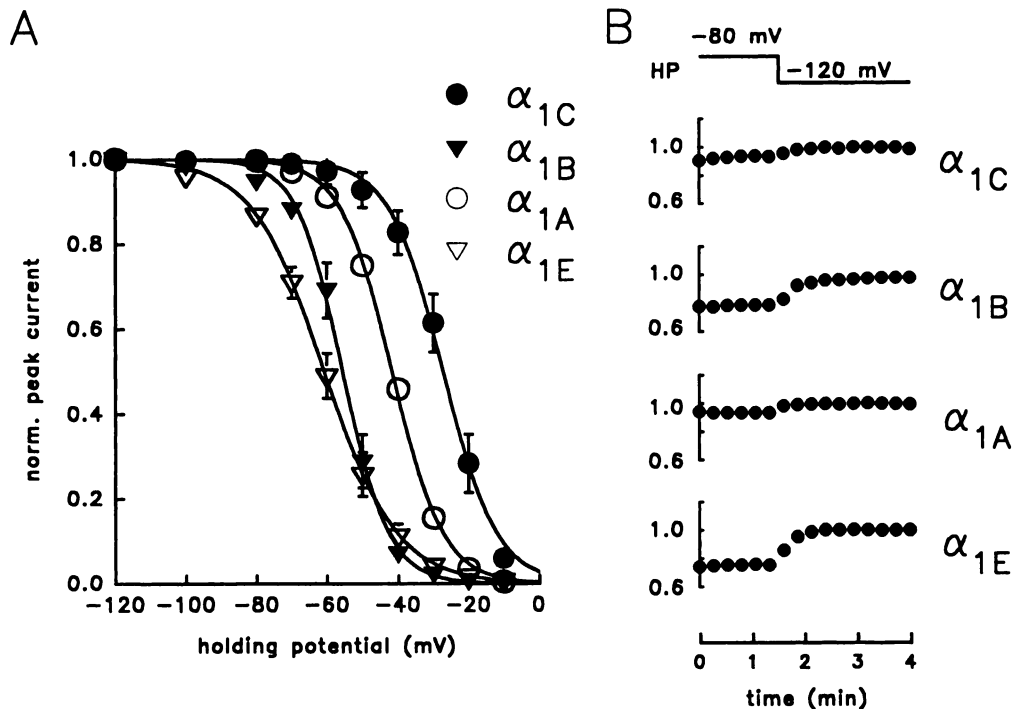
Fig. 5. Dependence of peak inward current on holding potential. A, Cumulative Ca^{2+} channel inactivation curve obtained by varying the holding potential between -120 mV and -10 mV. The holding potential was maintained for 1 min at each level. Mean amplitudes of peak currents evoked by two depolarizing test pulses from every holding potential were expressed as a fraction of the peak current evoked from a holding potential of -120 mV. The test potential was not changed in the course of the experiment and was set at 0 mV (α_{1C}, α_{1B}, and α_{1A}) or $+10$ mV (α_{1E}). Each point corresponds to the average (mean ± standard error) of the normalized data from at least three independent experiments for each type of subunit. The data were fit with a Boltzmann relationship: $I(V)/I(-120) = 1/(1 + \exp[(V - V_{1/2})/k])$. Curves, best fits to the data with values of $V_{1/2}$ equal to -27 mV ($\alpha 1C$), -55 mV ($\alpha 1B$), -42 mV ($\alpha 1A$), and -61 mV ($\alpha 1E$). B, Fraction of channels inactivated at -80 mV under conditions more closely approximating a true steady state. The fraction of the channels in the inactivated state at -80 mV was revealed by a sustained change in holding potential to -120 mV. Peak inward currents measured using depolarizing test pulses every 15 sec were normalized to the steady state value of the peak current at -120 mV holding potential in the same experiment and plotted against time. Only the segments of representative experiments for each clone corresponding to 6 pulses (90 sec) before and 10 pulses (150 sec) after the change in holding potential are shown. The test potential was set at 0 mV for all $\alpha 1$ subunits. The data from a representative experiment for each channel type are shown.

TABLE 1

Application of modulated receptor hypothesis to the analysis of mibefradil-inhibitory effect on calcium channels at different holding potentials

Affinities for mibefradil of resting (K_r) and inactivated (K_i) states of all four channel types were calculated based on the measurements performed at holding potentials -120 and -80 mV as explained in the text (eqs. 1-4).

Subunit type	q(-120 mV) (10 μM)	K_d(-80 mV)	h_∞(-80 mV)	K_r	K_i
		μM			μM
$\alpha 1C$	0.89	21.0	0.95	81	1.4
$\alpha 1B$	0.86	3.1	0.75	61	0.81
$\alpha 1A$	0.80	6.3	0.90	40	0.73
$\alpha 1E$	0.83	6.5	0.78	50	1.6

of inhibition was observed, but the initial rate of the drug washout was relatively slow. However, changing the holding potential from -80 mV to -120 mV yielded an immediate and marked increase in the rate of current recovery (Fig. 6). The k_{off} of mibefradil at holding potentials of -80 mV and -120 mV was estimated from the initial slope of a plot of peak current versus time during the drug washout. For all neuronal clones (A-, B-, and E-type), $k_{off}(-80$ mV) was in the range of 0.1–0.15 min^{-1} and $k_{off}(-120$ mV) was $\sim$0.7–0.8 min^{-1}, i.e., almost 10-fold faster. For L-type channels, however, an increase was only 2-fold (from 0.7 min^{-1} to $\sim$1.4 min^{-1}). These results are in apparent agreement with modulated receptor hypothesis if one assumes that at holding

potential of -80 mV, mibefradil is predominantly bound to the inactivated state of neuronal channels, which shows higher affinity for the drug and allows a slower rate of dissociation. We should point out, however, that these estimates are very approximate because of limitations in the speed of the solution change and the time resolution of the test pulses.

Mibefradil speeds decay of Ca^{2+} channel current. As illustrated in Fig. 7, mibefradil produced changes in the waveform of the Ba^{2+} currents. The traces show currents evoked by 150-msec test pulses, normalized with respect to the peak inward current and averaged across several different experiments. Averaged waveforms in the absence of drug and in the presence of 10 μM mibefradil are superimposed for each of the four channel types. As is evident, Ba^{2+} currents decayed more rapidly in the presence of mibefradil. These impressions were corroborated by quantitative analysis of the extent of decay during 150-msec test pulse (percent decay, Fig. 7B). Mibefradil caused a significantly greater degree of decay in all cases.

The effect of mibefradil on current waveform is reminiscent of the actions of dihydropyridines and verapamil on L-type channels; such effects have been attributed to drug binding to the open state (38). The hypothesis that mibefradil engages in interactions with open Ca^{2+} channels gains additional support from analysis of changes in current waveform on application of the drug (Fig. 8). The main result is illus-
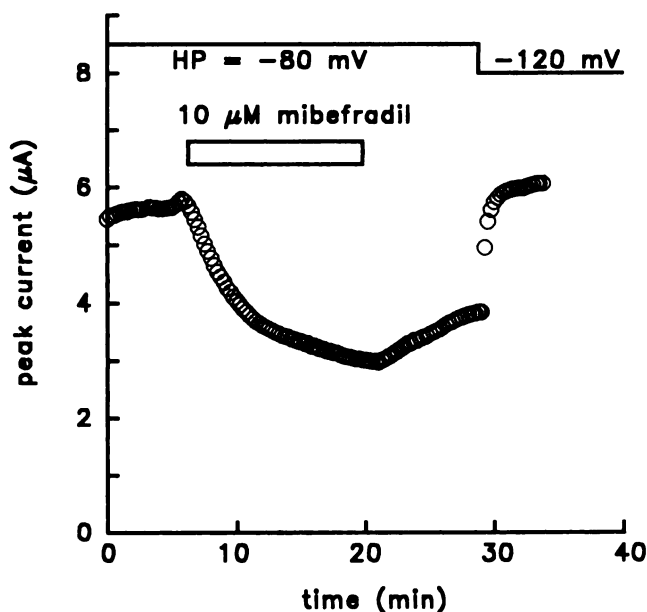
Fig. 6. Effect of holding potential (*HP*) on rate of washout of mibefradil effect. Inward currents were evoked by 50-msec test pulses to 0 mV every 15 sec. Peak currents are plotted against time. A change in holding potential from −80 mV to −120 mV during the washout of mibefradil causes an immediate and marked increase in the rate of current recovery. Data from a representative experiment with the α1A subunit are shown; qualitatively similar results were obtained with other subunits.

trated with records generated by the α1B clone, but similar results were obtained with other α1 subunits. Application of 10 μM mibefradil caused a decline in the peak current that began immediately on addition of the drug but required ~3 min to reach a new steady state (Fig. 8). However, the change in current waveform was fully evident immediately after addition of the drug (Fig. 8). Thus, the acceleration of the current decay is determined by the presence of the drug during test pulse rather than by the cumulative fraction of channels inhibited by the drug. These observations are consistent with the hypothesis that mibefradil can interact with the channel in its open state, thereby preventing further current flow. In effect, the open to open/blocked transition introduces a pathway in parallel with the open to inactivated step, thus giving the appearance of more rapid inactivation. An alternative mechanism could be a preferential binding of the drug to the open state of the channel, which causes an increase in the rate of channel inactivation through an allosteric effect. Analysis of macroscopic currents does not readily allow discrimination between these two models.

The impact of an additional pathway leading away from the conducting state would be expected to be most striking when the normal inactivation process was slow and least obvious when it was fast. This appears to be consistent with data for the various α1 subunits in Fig. 6; the increase in the percent decay was least obvious for α1E, possibly because it inactivated 3–4 times more rapidly than the other channel types in the absence of drug (see also Ref. 29).

Frequency dependence of mibefradil effect on L-type Ca^{2+} channels. On the basis of evidence that interactions of mibefradil with Ca^{2+} channels are promoted by channel opening and inactivation, it is to be expected that the effectiveness of the drug will depend strongly on the fre-
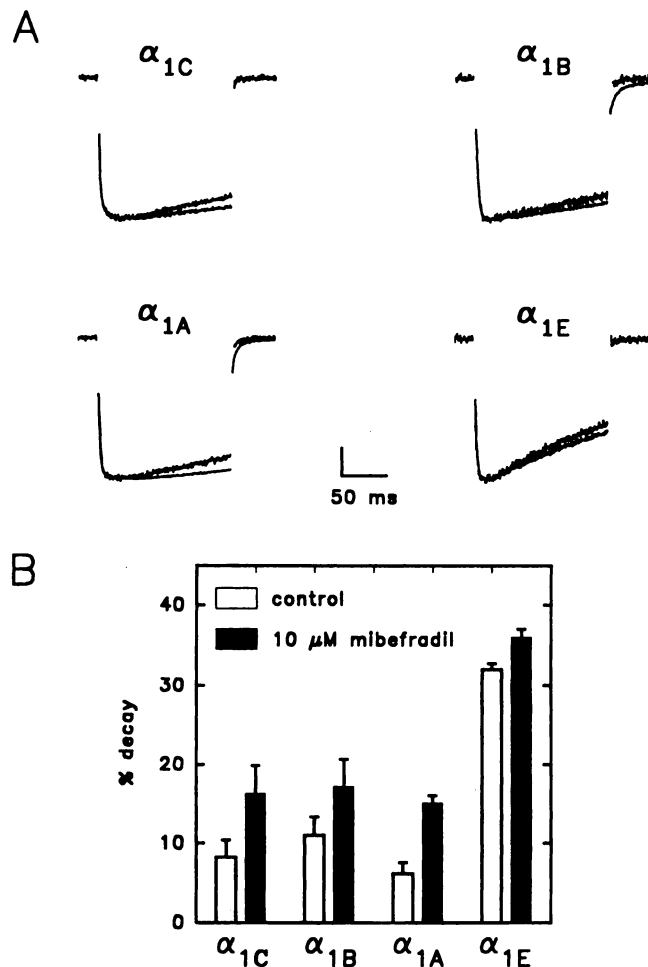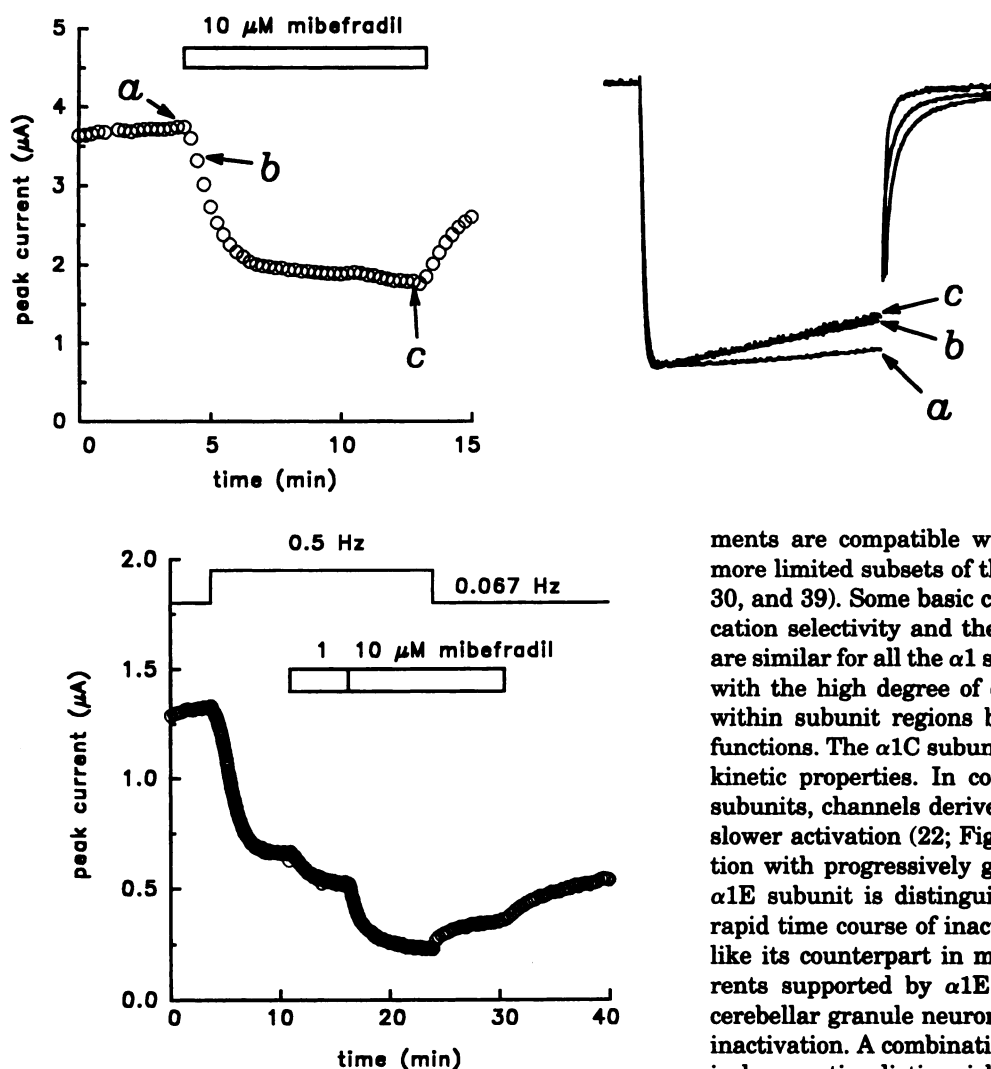

Fig. 7. Mibefradil hastens the decay of Ca^{2+} channel current. A, Comparison of averaged waveforms of inward current in the presence of 10 μM mibefradil and in the absence of drug. For all four channel types, currents were evoked by a 150-msec pulse from a −80 mV holding potential to 0 mV. Current traces from individual experiments were normalized according to the peak current and then averaged together. Each waveform represents compiled results from at least three experiments. Vertical scale bar, 20% of the peak current size. B, Degree of decline from peak current at the end of the 150-msec test pulse (percent decay) calculated for each subunit. Open bars, Absence of drug; shaded bars, presence of 10 μM mibefradil. Shown are values of mean ± standard error from at least four independent experiments with each subunit type.

quency of depolarization. This might be especially important for cardiac tissue at physiologically relevant heart rates. By comparison, blockade of L-type Ca^{2+} channels by mibefradil is likely to be underestimated at the low rates of stimulation (typically, 4 min^{-1}) used in the majority of the present study. Accordingly, we carried out experiments to examine the sensitivity of L-type channels at a higher frequency of depolarizing pulses. Fig. 9 shows an experiment with expressed α1C subunits at a holding potential of −80 mV. Mibefradil was delivered during a period of continuous stimulation at 0.5 Hz. At 1 μM, the drug caused substantial inhibition, which is in contrast to its relative ineffectiveness at a lower frequency of stimulation (Fig. 3). Increasing the mibefradil concentration to 10 μM caused further blockade. In the continued presence of 10 μM drug, lowering the frequency of stimulation to one pulse per 15 sec caused significant relief of inhibition (Fig. 9). The influence of stimulation frequency was consistently ob-

Fig. 8. The addition of mibefradil has an immediate effect on the current waveform. Peak inward currents, evoked by test pulses to 0 mV from holding potential of −80 mV every 15 sec, are plotted against time. The addition of 10 μM mibefradil inhibits the channels with a characteristic time course lasting several minutes. *a* through *c* indicate sweeps shown on the *right*, recorded just before the application of mibefradil (*a*) and 30 sec (*b*) and 9 min (*c*) after addition of the drug. Current waveforms were obtained by normalizing individual current signals by their peak current. Data shown for the α1B subunit are representative of results obtained with other subunits.

Fig. 9. Frequency dependence of mibefradil effect on L-type channels (α1C). Peak inward currents evoked by test pulses to 0 mV from a holding potential of −80 mV are plotted against time. Indicated are an increase in frequency of stimulation from one pulse every 15 sec (0.067 Hz) to one pulse every 2 sec (0.5 Hz) and application of 1 μM and 10 μM mibefradil.

served. Application of 1 μM mibefradil caused an inhibition of 12.3 ± 4.6% (three experiments) at a frequency of one pulse every 2 sec compared with 5.6 ± 1.0% (five experiments) with depolarizations once every 15 sec. Correspondingly, exposure to 10 μM mibefradil caused inhibition of 51.0 ± 7.2% (three experiments) and 31.7 ± 2.6% (five experiments) at the higher and lower rates of depolarization, respectively. Thus, mibefradil is significantly more potent as an inhibitor of L-type Ca^{2+} channels when the frequency of stimulation is elevated.

Discussion

Similarities and differences in biophysical properties of cloned α1 subunits. Our experiments provided a direct comparison of the functional properties of four classes of α1 subunits (C, B, A, and E), representing the major types of HVA Ca^{2+} channels (L-, N-, P/Q-, and R-type). This is the first study in which such a comparison has been made under identical conditions of expression. The results of our experi-

ments are compatible with previous comparisons between more limited subsets of these α1 subunits (e.g., Refs. 12, 22, 30, and 39). Some basic characteristics, such as the divalent cation selectivity and the voltage dependence of activation, are similar for all the α1 subunits (Fig. 2), which is consistent with the high degree of conservation of primary sequences within subunit regions believed to be important for these functions. The α1C subunit stands out with regard to certain kinetic properties. In comparison with class B, A, and E subunits, channels derived from the class C subunit exhibit slower activation (22; Fig. 1) and are less prone to inactivation with progressively greater depolarization (Fig. 5). The α1E subunit is distinguished from the others by its more rapid time course of inactivation (30, 40; Fig. 7), very much like its counterpart in marine ray (*doe-1*; 12, 30, 42). Currents supported by α1E are similar to R-type current in cerebellar granule neurons (8) with regard to the kinetics of inactivation. A combination of biophysical and pharmacological properties distinguish all four classes of HVA α1 subunit from low-voltage-activated T-type channels (see later).

Generality of state-dependent block for multiple types of HVA Ca^{2+} channel. At micromolar levels, mibefradil inhibited divalent currents generated by each of the classes of α1 subunits. In all cases, the effectiveness of the drug was enhanced at more depolarized holding potentials. The observations for L-type currents are in good agreement with earlier studies of mibefradil effects in isolated cardiomyocytes (19) and Chinese hamster ovary cells expressing α1C (21). What is particularly interesting is the presence of voltage dependence of block across the entire spectrum of HVA Ca^{2+} channels, not just for L-type channels. Mibefradil provides the first clear-cut example of how all the major classes of HVA Ca^{2+} channels can be blocked in a voltage-dependent manner.

As in the classic modulated receptor hypothesis (32, 34, 36, 37), we interpreted the dependence on steady depolarizations in terms of preferential binding to the channel's inactivated state. This led to quantitative estimates of the dissociation constants for mibefradil binding to resting and inactivated states of the individual channel types (Table 1). In all cases, the dissociation constants for the inactivated state lie in the range of 0.7–1.6 μM, concentrations ~50-fold lower than the K_d values for the resting state. The analysis emphasizes the point that apparent differences among various channel types

may arise simply from quantitative differences in gating, e.g., in the voltage or time dependence of inactivation or activation. For example, although it appears at first that cardiac channels were less sensitive than neuronally derived channel types to inhibition by mibefradil (Fig. 3), the apparent difference can be in large part explained by the fact that L-type channels show much less inactivation at the standard holding potential of −80 mV, thereby limiting the contribution of the inactivated state to the overall affinity. Likewise, some significant changes in sensitivity to mibefradil would be expected if the same α1 clone were coexpressed with different β subunits, simply because these also influence the voltage dependence of steady state inactivation. This mechanism may contribute to recently reported variations in sensitivity to mibefradil when cardiac α1C subunit was coexpressed with β1 or β3 subunit in Chinese hamster ovary cells (42). Thus, tissue-specific expression of Ca^{2+} channel auxiliary subunits (43) may contribute to differences among various organs in their physiological responses to mibefradil. Possible confounding effects of α2 and β subunits were minimized in our experiments by coexpression of different α1 subunits with the same complement of auxiliary subunits.

Experimental and clinical implications. Mibefradil provides a welcome addition to the pharmacological agents presently available for blocking non-L-type channels, which include diphenylalkylamines, diphenylbutylpiperidines (16), and peptide toxins (7). Some of these toxins, including ω-CTx GVIA, have extraordinary selectivity for particular types of Ca^{2+} channels, but they are often difficult to obtain in suitable quantity and to deliver to central nervous system targets. It seems likely that the mechanism of mibefradil action differs from that of ω-CTx GVIA, which is believed to act as a simple pore blocker (25, 44). Lack of specificity among the various HVA channels will be a drawback of mibefradil for many applications. We do not know if the drug interacts with similar or identical molecular determinants on the various types of channels or, if certain structural features are shared, whether further improvement of selectivity can be achieved. It is interesting to note that voltage dependence of mibefradil's effect on HVA channels is very similar to the voltage dependence of fluspirilene action on P-type channels (14), although these drugs are not structurally related. Nevertheless, the information on mibefradil's pattern of action offers general encouragement for efforts in developing drugs with specificity for N-, P-, Q-, or R-type channels, much as nifedipine has for L-type channels.

The specificity of mibefradil may already be sufficient to help in discriminating between T-type channels and HVA channels, including those encoded by α1E. T-type channels appear to be very sensitive to this drug, particularly in vascular smooth muscle cells, where 50% inhibition of T-type channels was obtained at 0.1 μM (20). T-type currents in neuroblastoma cells appear to be somewhat less sensitive, with an IC_{50} of ~1 μM (45). A more qualitative difference, perhaps a more fundamental one, lies in the influence of membrane potential. Although block of currents arising from α1E is strongly voltage dependent, as discussed, T-type channels appear to be blocked to a rather similar degree at different holding potentials (21). This adds to the growing body of evidence that T-type channels are distinct from those encoded by α1E (30).

The strong voltage dependence of mibefradil's action on

HVA channels may be at least partially responsible for its favorable profile as an emerging therapeutic agent. This compound appears to be very effective in blocking Ca^{2+} entry in tissues with less-negative resting potential, such as vascular smooth muscle and sinoatrial node, in keeping with its potent effects on T-type channels or partially inactivated L-type channels. On the other hand, mibefradil largely spares the Ca^{2+} delivery in tissues such as working myocardium, where the more-negative diastolic potentials favor the resting state of L-type channel, which is not very sensitive to inhibition by the drug. Thus, observations at the single-cell level help provide an explanation for the ability of mibefradil to decrease blood pressure and heart rate with a minimal negative inotropic effect, as observed in clinical trials (17).

References

1. Bean, B. P. Classes of calcium channels in vertebrate cells. *Annu. Rev. Physiol.* **51**:367–384 (1989).
2. Hess, P. Calcium channels in vertebrate cells. *Annu. Rev. Neurosci.* **13**: 1337–1356 (1990).
3. Tsien, R. W., D. Lipscombe, D. V. Madison, K. P. Bley, and A. P. Fox. Multiple types of neuronal calcium channels and their selective modulation. *Trends Neurosci.* **11**:431–438 (1988).
4. Tsien, R. W., and R. Y. Tsien. Calcium channels, stores and oscillations. *Annu. Rev. Cell. Biol.* **6**:715–760 (1990).
5. Bertolino, M., and R. R. Llinas. The central role of voltage-activated and receptor-operated calcium channels in neuronal cells. *Annu. Rev. Pharmacol. Toxicol.* **32**:399–421 (1992).
6. Bean, B. P., and I. M. Mintz. Pharmacology of different types of calcium channels in rat neurons, in *Handbook of Membrane Channels* (C. Peracchia, ed.). Academic Press, San Diego, 199–212 (1994).
7. Olivera, B. M., G. P. Miljanich, J. Ramachandran, and M. E. Adams. Calcium channel diversity and neurotransmitter release: the *omega*-conotoxins and *omega*-agatoxins. *Annu. Rev. Biochem.* **63**:823–867 (1994).
8. Randall, A., and R. W. Tsien. Pharmacological dissection of multiple types of Ca^{2+} channel currents in rat cerebellar granule neurons. *J. Neurosci.* **15**:2995–3012 (1995).
9. Snutch, T. P., and P. B. Reiner. Ca^{2+} channels: diversity of form and function. *Curr. Opin. Neurobiol.* **2**:247–253 (1992).
10. Tsien, R. W., P. T. Ellinor, and W. A. Horne. Molecular diversity of voltage-dependent Ca^{2+} channels. *Trends Pharm. Sci.* **12**:349–354 (1991).
11. Mori, Y. Molecular biology of voltage-dependent calcium channels, in *Handbook of Membrane Channels* (C. Peracchia, ed.). Academic Press, San Diego, 163–176 (1994).
12. Zhang, J.-F., A. D. Randall, P. T. Ellinor, W. A. Horne, W. A. Sather, T. Tanabe, T. L. Schwarz, and R. W. Tsien. Distinctive pharmacology and kinetics of cloned neuronal Ca^{2+} channels and their possible counterparts in mammalian CNS neurons. *Neuropharmacology* **32**:1075–1088 (1993).
13. Kass, R. S. Molecular pharmacology of cardiac L-type calcium channels, in *Handbook of Membrane Channels* (C. Peracchia, ed.). Academic Press, San Diego, 187–198 (1994).
14. Sah, D. W. Y., and B. P. Bean. Inhibition of P-type and N-type calcium channels by dopamine receptor antagonists. *Mol. Pharmacol.* **45**:84–92 (1994).
15. Grantham, C. J., M. J. Main, and M. B. Cannell. Fluspirilene block of N-type calcium current in NGF-differentiated PC12 cells. *Br. J. Pharmacol.* **111**:483–488 (1994).
16. Spedding, M., B. Kenny, and P. Chatelain. New drug binding sites in Ca^{2+} channels. *Trends Pharmacol. Sci.* **16**:139–142 (1995).

17. Clozel, J.-P., W. Osterrieder, C. H. Kleinbloesem, H. A. Welker, B. Schlappi, R. Tudor, F. Hefti, R. Schmitt, and H. Eggers. Ro 40–5967: a new nondihydropyridine calcium antagonist. *Cardiovasc. Drug Rev.* 9:4–17 (1991).

18. Osterrieder, W., and M. Holck. *In vitro* pharmacologic profile of Ro 40–5967, a novel Ca²⁺ channel blocker with potent vasodilator but weak inotropic action. *J. Cardiovasc. Pharmacol.* 13:754–759 (1989).

19. Liang-min, F., and W. Osterrieder. Potential-dependent inhibition of cardiac Ca²⁺ inward currents by Ro 40–5967 and verapamil: relation to negative inotropy. *Eur. J. Pharmacol.* 196:205–207 (1991).

20. Mishra, S. K., and K. Hermsmeyer. Selective inhibition of T-type Ca²⁺ channels by Ro 40–5967. *Circ. Res.* 75:144–148 (1994).

21. Mehrke, G., X. G. Zong, V. Flockerzi, and F. Hofmann. The Ca⁺⁺-channel blocker Ro 40–5967 blocks differently T-type and L-type Ca⁺⁺ channels. *J. Pharmacol. Exp. Ther.* 271:1483–1488 (1994).

22. Sather, W. A., T. Tanabe, J.-F. Zhang, Y. Mori, M. E. Adams, and R. W. Tsien. Distinctive biophysical and pharmacological properties of class A (BI) calcium channel α1 subunits. *Neuron* 11:291–303 (1993).

23. Titus, D. E., ed. *Protocols and Applications Guide.* Ed. 2. Promega, Madison, WI (1991).

24. Mikami, A., K. Imoto, T. Tanabe, T. Niidome, Y. Mori, H. Takeshima, S. Narumiya, and S. Numa. Primary structure and functional expression of the cardiac dihydropyridine-sensitive calcium channel. *Nature (Lond.)* 340:230–233 (1989).

25. Ellinor, P. T., J.-F. Zhang, W. A. Horne, and R. W. Tsien. Structural determinants of the blockage of N-type calcium channels by a peptide neurotoxin. *Nature (Lond.)* 372:272–275 (1994).

26. Mori, Y., T. Friedrich, M.-S. Kim, A. Mikami, J. Nakai, P. Ruth, E. Bosse, F. Hofmann, V. Flockerzi, T. Furuichi, K. Mikoshiba, K. Imoto, T. Tanabe, and S. Numa. Primary structure and functional expression from complementary DNA of a brain calcium channel. *Nature (Lond.)* 350:398–402 (1991).

27. Hullin, R., D. Singer-Lahat, M. Freichel, M. Biel, N. Dascal, F. Hofmann, and V. Flockerzi. Calcium channel beta subunit heterogeneity: functional expression of cloned cDNA from heart, aorta and brain. *EMBO J.* 11:885–890 (1992).

28. Williams, M. E., P. F. Brust, D. H. Feldman, S. Patthi, S. Simerson, A. Maroufi, A. F. McCue, G. Velicelebi, S. B. Ellis, and M. M. Harpold. Structure and functional expression of an omega-conotoxin-sensitive human N-type calcium channel. *Science (Washington D. C.)* 257:389–395 (1992).

29. Ellinor, P. T., J.-F. Zhang, A. D. Randall, M. Zhou, T. Schwarz, R. W. Tsien, and W. A. Horne. Functional expression of a rapidly inactivating neuronal calcium channel. *Nature (Lond.)* 363:455–458 (1993).

30. Williams, M. E., L. M. Marubio, C. R. Deal, M. Hans, P. F. Brust, L. H. Philipson, R. J. Miller, E. C. Johnson, M. M. Harpold, and S. B. Ellis. Structure and functional characterization of neuronal α1E calcium channel subtypes. *J. Biol. Chem.* 269:22347–22357 (1994).

31. Kass, R. S., and M. C. Sanguinetti. Calcium channel inactivation in the cardiac Purkinje fiber: evidence for voltage- and calcium-mediated mechanisms. *J. Gen. Physiol.* 84:705–726 (1984).

32. Bean, B. P. Nitrendipine block of cardiac calcium channels: high affinity binding to the inactivated state. *Proc. Natl. Acad. Sci. USA* 81:6388–6392 (1984).

33. Kokubun, S., B. Prod'hom, C. Becker, H. Porzig, and H. Reuter. Studies on Ca²⁺ channels in intact cardiac cells: voltage-dependent effects and cooperative interactions of dihydropyridine enantiomers. *Mol. Pharmacol.* 30: 571–584 (1987).

34. Hille, B. Local anesthetics: hydrophilic and hydrophobic pathways for the drug-receptor reaction. *J. Gen. Physiol.* 69:497–515 (1977).

35. Hille, B. *Ionic Channels of Excitable Membranes.* Sinauer Associates, Sunderland, MA (1992).

36. Hondeghem, L. M., and B. G. Katzung. Time- and voltage-dependent interactions of antiarrhythmic drugs with cardiac sodium channels. *Biochim. Biophys. Acta* 472:373–398 (1977).

37. Bean, B. P., C. J. Cohen, and R. W. Tsien. Lidocaine block of cardiac sodium channels. *J. Gen. Physiol.* 81:613–642 (1983).

38. Lee, K. S., and R. W. Tsien. Mechanism of calcium channel blockade by verapamil, D600, diltiazem and nitrendipine in single dialysed heart cells. *Nature (Lond.)* 302:790–794 (1983).

39. Stea, A., J. W. Tomlinson, T. W. Soong, E. Bourinet, S. J. Dubel, S. R. Vincent, and T. P. Snutch. Localization and functional properties of a rat brain alpha₁ₐ calcium channel reflect similarities to neuronal Q- and P-type channels. *Proc. Natl. Acad. Sci. USA* 91:10576–10580 (1994).

40. Soong, T. W., A. Stea, C. D. Hodson, S. J. Dubel, S. R. Vincent, and T. P. Snutch. Structure and functional expression of a member of the low voltage-activated calcium channel family. *Science (Washington D. C.)* 260: 1133–1136 (1993).

41. Zhang, J.-F., P. T. Ellinor, R. W. Aldrich, and R. W. Tsien. Molecular determinants of voltage-dependent inactivation in calcium channels. *Nature (Lond.)* 372:97–100 (1994).

42. Welling, A., L. Lacinova, K. Donatin, A. Ludwig, E. Bosse, V. Flockerzi, and F. Hofmann. Expression of the L-type calcium channel with two different β subunits and its modulation by Ro 40–5967. *Pflugers Arch.* 429:400–411 (1995).

43. Isom, L. L., K. S. De Jongh, and W. A. Catterall. Auxiliary subunits of voltage-gated ion channels. *Neuron* 12:1183–1194 (1994).

44. Boland, L. M., J. A. Morrill, and B. P. Bean. omega-Conotoxin block of N-type calcium channels in frog and rat sympathetic neurons. *J. Neurosci.* 14:5011–5027 (1994).

45. Randall, A. D. A biophysical and pharmacological comparison of R- and T-type calcium channels. *J. Physiol.*, in press.